Supplemental Information

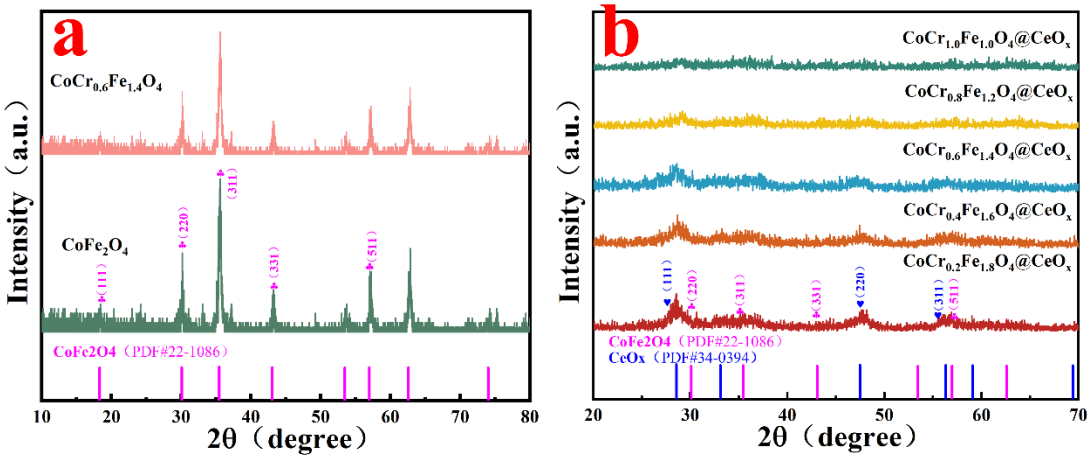

Fig. S1 XRD spectra of the catalyst (a) $CoFe_2O_4$ and $CoCr_{0.6}Fe_{1.4}O_4$, (b) $CoCr_yFe_{2-y}O_4@CeO_x$.

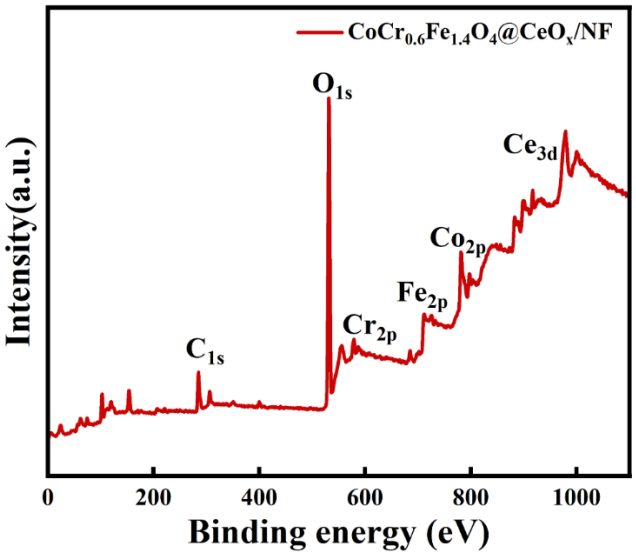

Fig. S2 XPS spectrum of $CoCr_{0.6}Fe_{1.4}O_4@CeO_x$.

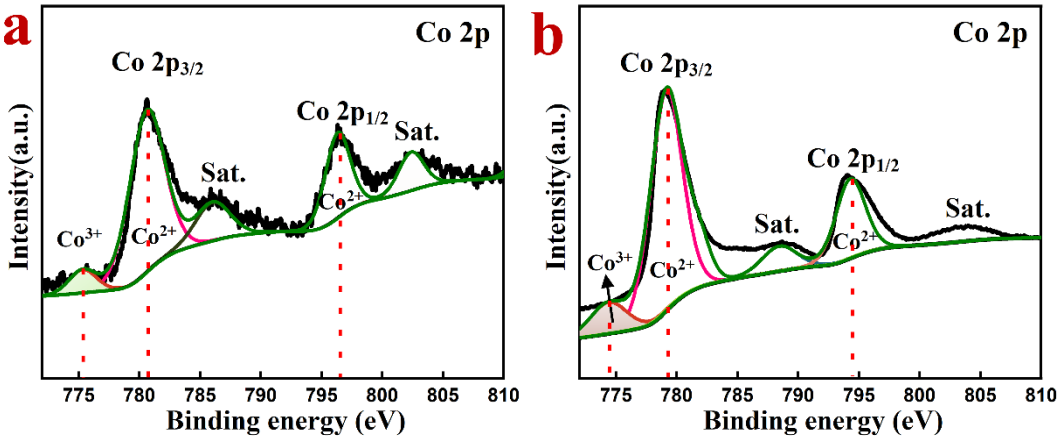

Fig. S3 Co 2p XPS spectra of different catalysts: (a) $CoFe_2O_4$, (b) $CoCr_{0.6}Fe_{1.4}O_4$.

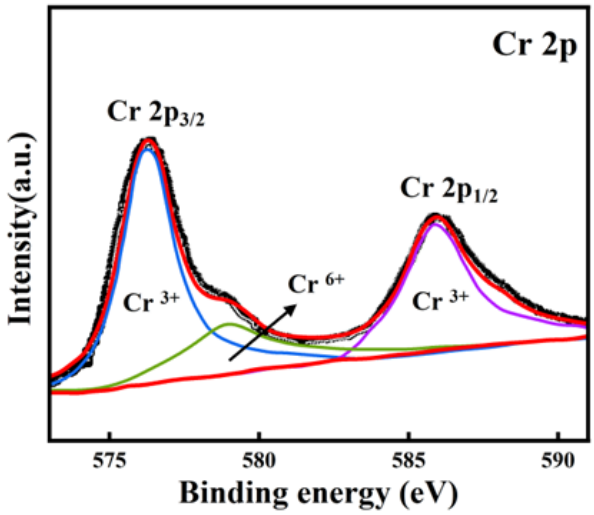

Fig. S4 XPS spectrum of Cr 2p in $CoCr_{0.6}Fe_{1.4}O_4$.

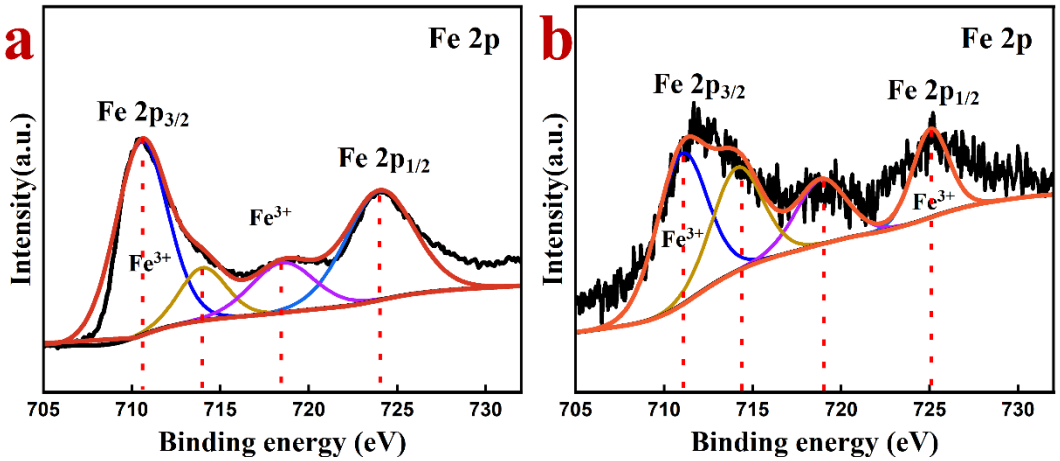

Fig. S5 Fe 2p XPS spectra of different catalysts: (a) $CoFe_2O_4$, (b) $CoCr_{0.6}Fe_{1.4}O_4$.

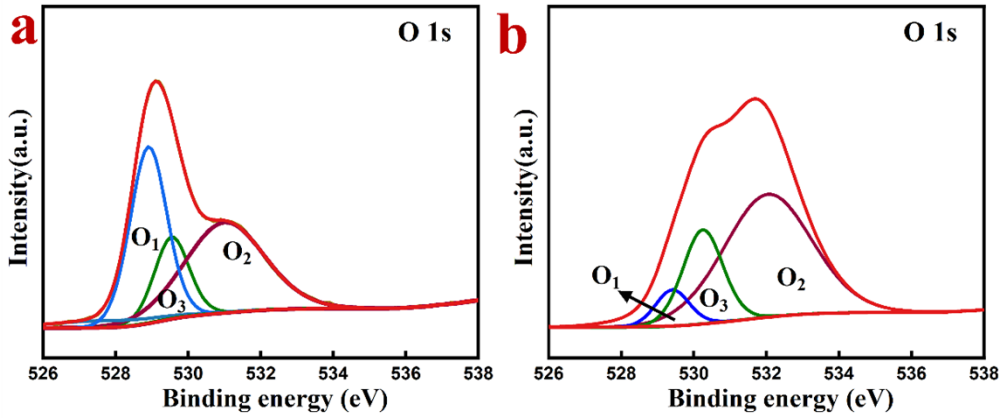

Fig. S6 O1s spectra of different catalysts: (a) $CoFe_2O_4$, (b) $CoCr_{0.6}Fe_{1.4}O_4$.

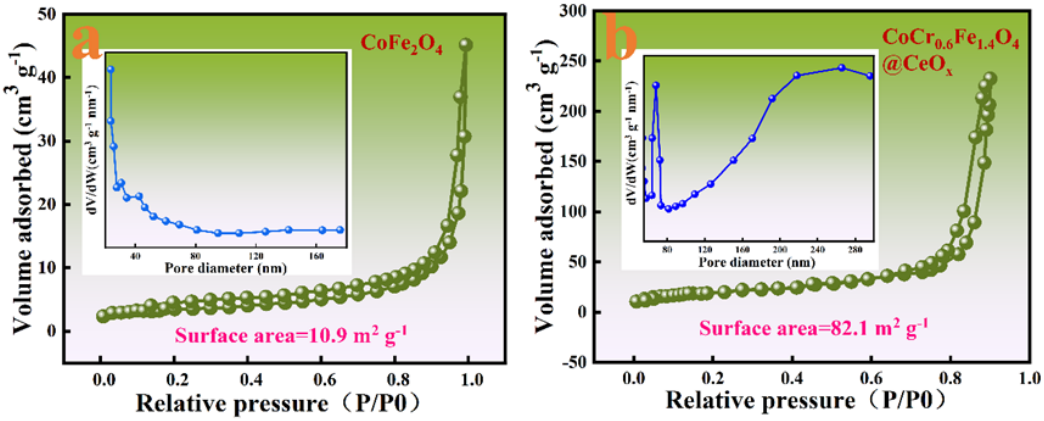

Fig. S7 Nitrogen adsorption-desorption isotherm and pore-size distribution of (a) $CoFe_2O_4$ and (b) $CoCr_{0.6}Fe_{1.4}O_4$@CeO_x.

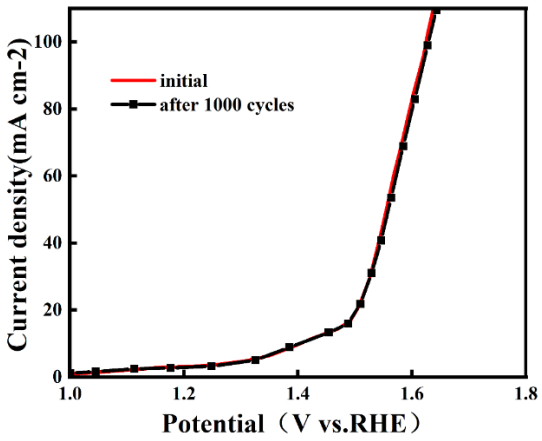

Fig. S8 Comparison of $CoCr_{0.6}Fe_{1.4}O_4$@CeO_x/NF after 1000 CV scans with the initial OER LSV curve.

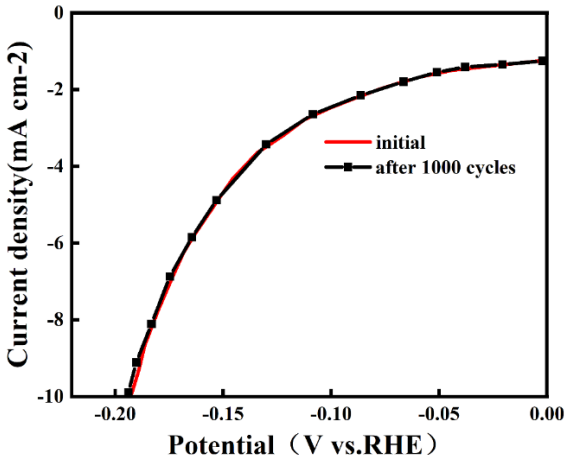

Fig. S9 Comparison of $CoCr_{0.6}Fe_{1.4}O_4$@CeO_x/NF after 1000 CV scans with the initial HER LSV curve.

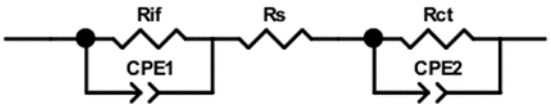

Fig. S10 Equivalent circuit at the electrode/electrolyte interface.

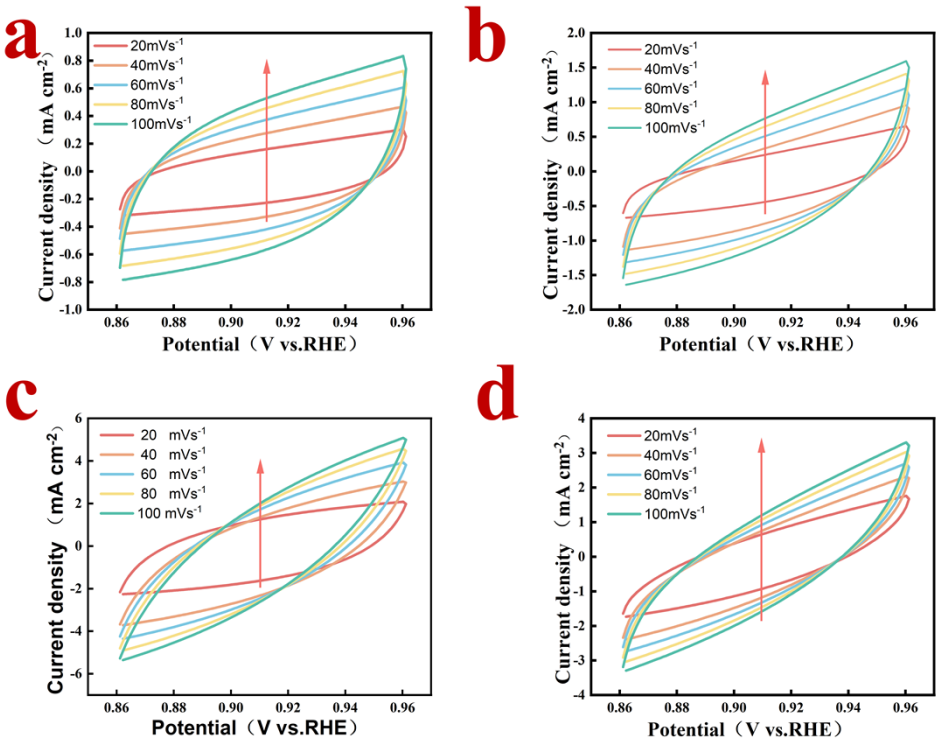

Fig. S11 CV curves measurements of different samples at various scan rates: (a) $CoCr_{0.6}Fe_{1.4}O_4$@CeO_x, (b) $CoCr_{0.6}Fe_{1.4}O_4$, (c) $CoFe_2O_4$, and (d) $CoCr_{0.8}Fe_{1.2}O_4$@CeO_x.

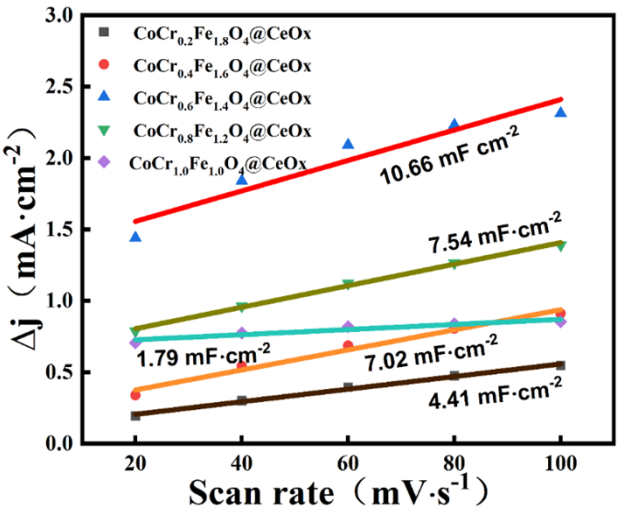

Fig. S12 Relationship between capacitive current density and scan rate for different $CoCr_yFe_{2-y}O_4@CeO_x$ electrodes.

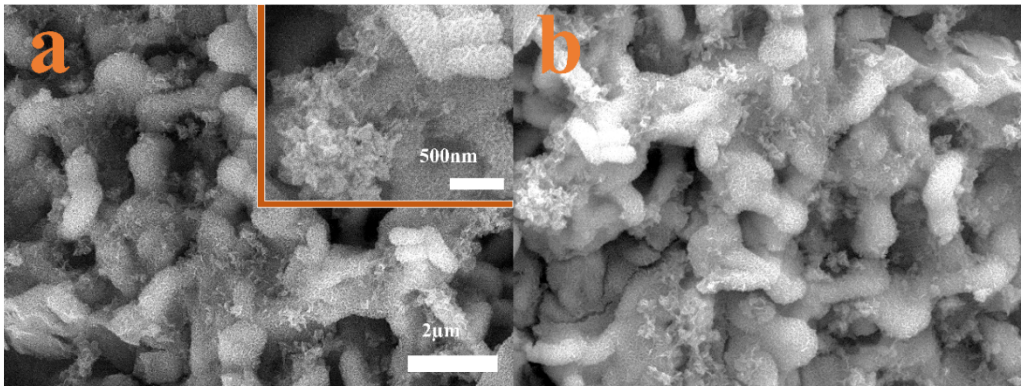

Fig. S13 SEM plot of $CoCr_{0.6}Fe_{1.4}O_4@CeO_x$/NF nanorods after OER reaction.

Table S1 Potentials (U) at 100 mA and conductivity (ρ) of different catalysts obtained by four-point probe device.

Materials	U1 (mV)	U2 (mV)	U3 (mV)	U4 (mV)	U5 (mV)	Average value of U (mV)	ρ (Ω·m)
$CoFe_2O_4$	25.17	30.43	27.43	26.81	26.87	27.34	2.10×10^{-3}
$CoCr_{0.6}Fe_{1.4}O_4$	12.14	14.11	11.34	11.45	12.89	12.39	9.53×10^{-4}

Supplementary Note 1

XRD sample preparation, the nickel foam loaded with the target sample is cut to 10 mm × 10 mm size for testing.

HR-TEM sample preparation, nickel foam is magnetic and the magnetism of the sample will affect the HR-TEM results, so to reduce the effect of nickel foam on HR-TEM results, we used physical stripping to collect a sufficient amount of powder samples and grind the powder samples to reduce the size. Then the appropriate amount of powder and ethanol were taken and added to a small beaker for ultrasonic oscillation for 30 min. After the end of ultrasonication, a homogeneous mixture of powder and ethanol was sucked up with a glass capillary tube, and then 2~3 drops of this mixture were dropped onto a microgrid (diameter 3 mm), and when the ethanol on the microgrid evaporated, it was ready to be tested.

XPS sample preparation and sample magnetism will affect the test results, so still selected powder samples for testing, using the physical stripping method to collect a sufficient amount of powder samples, and grinding of powder samples to reduce the size. The powder sample is then pressed with a tablet press, cut down to 5 mm × 5 mm size, and stuck to the XPS sample stage using conductive adhesive for testing.

Supplementary Note 2

Conductivity of samples before and after Cr doping by four-point probe method. To further reveal the conductivity before and after Cr doping, we measure the resistivity of $CoFe_2O_4$ and $CoCr_{0.6}Fe_{1.4}O_4$ by using the four-point probe method. First, the $CoFe_2O_4$ and $CoCr_{0.6}Fe_{1.4}O_4$ powders were respectively pressed into 2 × 2

cm^2 tablets, and their thickness is 0.2 cm. Then, these samples were measured their related potential at a certain current by using a four-point probe device (Shanghai Qianfeng Co., SQ120/2), and the resistivity values can be calculated by the following equation [1-4]:

$$\rho = C \cdot \frac{U}{I} \cdot W$$

Where the ρ is the resistivity, the U, I and W are the potential, current, and thickness of sample, the C is the corrective factor that is related to the shape and width of sample. In this work, the W is 0.2 cm, the I is 100 mA, and the C is 3.846 [3-5].

Supplementary Note 3

Hydrogen and oxygen evolution measurements:

The amount of H_2 produced on the $CoCr_{0.6}Fe_{1.4}O_4$@CeO_x/NF electrode at a constant current density of 20 $mA \cdot cm^{-2}$ in 1.0 M KOH was measured by using gas chromatography (GC, Tianmei Scheme 1 The procedure for the preparation of the $CoCr_{0.6}Fe_{1.4}O_4$@CeO_x/NF hybrid. 3301 company, GC7890II) with high purity N_2 (containing 2% CH_4) as carrier gas. The $CoCr_{0.6}Fe_{1.4}O_4$@CeO_x/NF electrode had a geometric area of of 1.0 cm × 0.5 cm. The electrolysis measurements were carried out in a special three-compartment electrochemical cell. The three compartments were connected at the bottom and the compartment for the working electrode had an air-inlet tube reaching to the bottom and a top opening that could be sealed from air with a rubber stopper. Before measurements, the electrolyte was bobbled with N_2 for 30 min to remove dissolved oxygen in solution and air in the compartments. The gas sample was taken from the working electrode chamber with a gas tight syringe through the sealed rubber cap at electrolysis time of 5, 10, 15, 20, 25, and 30 min. The evolution of H_2 was calculated out by integrating the peak area in GC spectra. The relationship between the peak area of H_2 in GC spectra and the actual H_2 amount was firstly calibrated using Pt electrode. The theoretically expected evolution of H_2 at constant j of 20 $mA \cdot cm^{-2}$ was calculated according to Faraday's law, and the Faradic efficiency for HER at working electrode was estimated by comparing the measured

and calculated values.

The amount of O_2 produced on the $CoCr_{0.6}Fe_{1.4}O_4$@CeO_x/NF electrode at a constant current density of 20 mA·cm^{-2} in 1.0 M KOH was measured by using O_2 fluorescence detector (Ocean Optics, R-sensor) in the working electrode compartment. Before measurements, the working electrode compartment was purged with N_2 for 30 min. During the oxygen evolution at a constant j of 20 mA·cm^{-2} for 30 min, the amount of O_2 on the $CoCr_{0.6}Fe_{1.4}O_4$@CeO_x/NF was directly measured by the O_2 sensor. The theoretically expected evolution of O_2 at constant j of 20 mA·cm^{-2} was calculated according to Faraday's law, and the Faradic efficiency for OER at working electrode was estimated by comparing the measured and calculated values.

References

[1] Chen. Y, Juang. J, Finite element analysis and equivalent parallel-resistance model for conductive multilayer thin films, Meas. Sci. Technol. 27 (2016) 074006

[2] Xue. J, Al-Dahhan. M, Dudukovic. M, Mudde. R, Four-point optical probe for measurement of bubble dynamics: Validation of the technique, Flow. Meas. Instrum. 19 (2008) 293-300.

[3] Tehrani. S, Lim. W, Lee. L, Correction factors for films resistivity measurement, Measurement. 45 (2012) 219-225.

[4] Dutta. B, Fahmy. N, Pegg. I, Effect of mixing transition ions in glasses. II. The P_2O_5-Fe_2O_3-MnO system, J. Non-cryst. Solids. 351 (2005) 2552-2561.

[5] Kleinlogel. C, Gauckler. L, Mixed electronic-ionic conductivity of cobalt doped cerium gadolinium oxide, J. Electroceram. 5 (2000) 231-243.